Journal of Applied Analysis and Computation
Volume 14, Number 1, February 2024, 146–161
Website:http://www.jaac-online.com
DOI:10.11948/20230104

CONVERGENT APPROACHES FOR THE DIRICHLET MONGE-AMPÈRE PROBLEM

Hajri Imen[1,†] and Fethi Ben Belgacem[2]

Abstract In this article, we introduce and study three numerical methods for the Dirichlet Monge-Ampère equation in two dimensions. The approaches consist in considering new equivalent problems. In the first method (method A) the equivalent problem is discretized by a wide stencil finite difference discretization and monotone schemes are obtained. Hence, we apply the Barles-Souganidis theory to prove the convergence of the schemes and the Damped Newtons method is used to compute the solutions of the schemes. In the last two methods (B and C) we introduce two fixed point operators. Finally, some numerical results are illustrated.

Keywords Monge-Ampère, fixed point, wide stencil, Newton method.

MSC(2010) 35J99, 65N06.

1. Introduction

We are interested in the numerical solution of the Monge-Ampère equation with Dirichlet boundary condition

$$\text{(MAD)} \begin{cases} \det\left(D^2 u\left(x\right)\right) = f\left(x\right), \ \text{for } x \text{ in } \mathit{\Omega}, \\ u\left(x\right) = \varphi\left(x\right), \ \text{for } x \text{ on } \partial\mathit{\Omega}, \\ u \text{ is convex.} \end{cases} \tag{1.1}$$

Where Ω is a convex bounded domain in $\mathbb{R}^2$, with boundary $\partial\mathit{\Omega}$, $\left(D^2 u\right)$, is the Hessian of the function u, f and φ are given functions.

For more general operator of Monge-Ampère and other boundary conditions, we mention for instance [29]. The convexity constraint is crucial for the (MAD). It is required for the Monge-Ampère equation to be degenerate elliptic and for (MAD) to have a unique solution. It is also needed for numerical stability. The Monge-Ampère equation, has extensive applications, it is strictly related to the "prescribed Gauss curvature" problem, see for instance [29]. It appears also in affine geometry, precisely, in the affine sphere problem and the affine maximal surfaces problem, this was discussed in [8, 9, 30, 33–36]. Other applications appear in fluid mechanics, geometric optics, and meteorology : for example, in semigeostrophic equations, the

†The corresponding author.
1 Department of Textile and Fashion Management, University of Monastir, Cornich 5000, Tunisia
2 Laboratory of partial differential equations (LR03ES04), ISIMM, University of Monastir, Cornich 5000, Tunisia
Email: hajri.imene2017@gmail.com(I. Hajri), fethi.benbelgacem@isimm.rnu.tn(F. B. Belgacem)

Monge-Ampère equation is coupled with a transport equation, this is pointed out in [29]. The analysis of the regularity of the Monge-Ampere equation is essential in the study of the regularity of the transport problem. This, latter, has been employed in many areas. We only briefly mention [7, 13, 15] for mesh geneartion, [19, 20, 31] for image registration, and [29] for reflector design. Developing an efficient numerical method has aroused a lot of interest, and large standard techniques have been proposed. A first method to do so was introduced in [28] by using a discretization of the geometric Alexandrov-Bakelman interpretation of solutions. Variational approaches have been presented in [10, 11], more precisely, the augmented Lagrangian approach and the least-squares approach. But these methods needed more regularity than can be predicted for solutions. A different approach was studied in [14], using the vanishing moment method. Methods using Newton's algorithm are discussed in [21, 22]. Numerical method based on the method of characteristics was discussed in [5]. We mention also the recent discretizations of the Monge-Ampere equation introduced in [4, 6, 21].

Although, the standard techniques, mentioned above, work well for smooth solutions they fail for singular solutions. As an illustration, in [12] the authors give an example of a solution that is not in $H^2(\Omega)$, for which their method diverges.

The standard finite difference discretization of the Monge-Ampère equation does not enforce the convexity condition and it can lead to instabilities. In addition, Newton's method may be unstable and there is no reason to consider that the standard discretization converges. In particular, the two dimensional scheme may have multiple solutions. For more details, see, for instance, the discussion in [3]. To overcome these difficulties, we have to use the notion of viscosity solution or Alexsandrov solution. In two dimension, a numerical method was introduced in [28], which is geometric in nature, and converges to the Alexsandrov solution. The method introduced in [26] in two dimension and improved in [16] for higher dimension (see also [23] in the same context), uses the wide stencil scheme that converges to the viscosity solution. We note also that consistency and stability of the numericals methods for the Monge-Ampère equation is not sufficient to prove convergence to the viscosity solution. For convergence, monotonicity is also needed. In this setting, building monotone methods requires the use of wide stencils.

The approaches that we consider in the present paper are inspired by the idea developed in [2] and the wide stencil finite difference discretization introduced in [26] for viscosity solution of M-A equation. This discretization relies on a framework developed in [1]. For clarity, we recall the full result in the next section.

2. Viscosity solution and convergence theory of approximation schemes

2.1. Degenerate elliptic equations

Let $F(x, r, p, X)$ be a continuous real valued function defined on $\Omega \times \mathbb{R} \times \mathbb{R}^n \times S^n$, with S^n being the space of symmetric $n \times n$ matrices. Consider the nonlinear, partial differential equation with Dirichlet boundary conditions,

$$\begin{cases} F\left(x, u(x), Du(x), D^2u(x)\right)(x) = 0 & \text{for } x \text{ in } \Omega, \\ u(x) = g(x) & \text{for } x \text{ in } \partial\Omega. \end{cases}$$

Where Ω is a domain in $\mathbb{R}^n$, Du and D^2u denote the gradient and Hessian of u, respectively.

Definition 2.1 ([16])**.** The equation F is degenerate elliptic if

$$F\left(x,r,p,X\right)\leq F\left(x,s,p,Y\right) \text{ whenever } r\leq s \text{ and } Y\leq X.$$

Where $Y\leq X$ means that $Y-X$ is a nonnegative definite symmetric matrix.

The viscosity solution for the Monge-Ampère equation is defined in [26].

Definition 2.2. Let $u\in C\left(\Omega\right)$ be convex and $f\geq 0$ be continuous. The function u is a viscosity subsolution (supersolution) of the Monge-Ampère equation in Ω if whenever convex $\varphi\in C^2\left(\Omega\right)$ and $x_0\in\Omega$ are such that $\left(u-\varphi\right)\left(x\right)\leq\left(\geq\right)\left(u-\varphi\right)\left(x_0\right)$ for all x in a neighborhood of x_0, then we must have

$$\det\left(D^2\phi\left(x_0\right)\right)\geq\left(\leq\right)f\left(x_0\right).$$

The function u is a viscosity solution if it is both a viscosity subsolution and supersolution.

For the existence and uniqueness of viscosity solution for (1.1), we mention the next result in [18],

Theorem 2.1. *Let $\Omega\subseteq\mathbb{R}^d$ be abounded and strictly convex, $g\in C\left(\partial\Omega\right)$, $f\in C\left(\Omega\right)$, with $f\geq 0$. Then there exists a unique convex viscosity solution $u\in C\left(\bar{\Omega}\right)$ of the problem (1.1).*

The advantage of considering viscosity solutions come from the following fundamental theorem, obtained in [1], which gives conditions for convergence of approximation schemes to viscosity solution.

Theorem 2.2. *(Convergence of Approximation Schemes). Consider a degenerate elliptic equation, for which there exist unique viscosity solutions. A consistent, stable approximation scheme converges uniformly on compact subsets to the viscosity solution, provided it is monotone.*

By the previous theorem, we need just a way to build a monotone finite difference schemes, which represents a new challenge. In the sequel, we recall here the basic framework introduced in [24], for building a monotone scheme.

Firstly, a finite difference equation take the form

$$F^i\left[u\right]=F^i\left(u_i,u_i-u_j|_{i\neq j}\right).$$

We say that a scheme is degenerate elliptic if the following holds [24]:

Definition 2.3. The scheme F is degenerate elliptic if F^i is non-decreasing in each variable.

We are now ready to present the following theorem in [24]:

Theorem 2.3. *Under mild analytic conditions, degenerate elliptic schemes are monotone, and non-expansive in the uniform norm. The iteration*

$$u^{m+1}=u^m+dtF\left(u^m\right), \tag{2.1}$$

is a contraction in L^∞ provided $dt\leq K\left(F\right)^{-1}$, where $K\left(F\right)$ is the Lipschitz constant of the scheme, regarded as a function from $\mathbb{R}^N\longrightarrow\mathbb{R}^N$.

We end this paragraph by the next result, proven in [24].

Theorem 2.4. *A proper, locally Lipschitz continuous degenerate elliptic scheme has a unique solution which is stable in the l^∞ norm.*

We finish this section by noting that wide stencil schemes are required to build consistent, monotone schemes of degenerate second order PDEs (see discussion in [26]). Wide stencil schemes were built for the two-dimensional Monge-Ampère equation in [26] and for the convex envelope in [25]. Each approach considered here is a function of eigenvalues of the Hessian. To fully discretize the equation (4.1) for the eigenvalues of the Hessian on a finite difference grid, we approximate the second derivatives by centered finite differences; this is the spatial discretization, with parameter h. We consider also a finite number of possible directions ν that lie on the grid; this is the directional discretization, with parameter $d\theta$. The spatial resolution is improved by using more grid points, the directional resolution is improved by increasing the size of the stencil. So, a wide stencil is needed (see Fig 1). This article is structured as follows: in Section 3, we introduce a new formulation

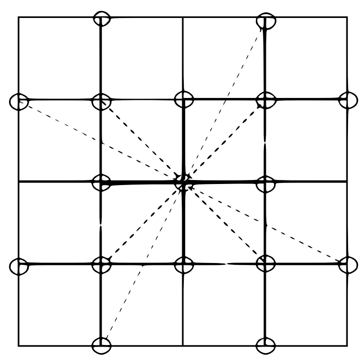

Figure 1. Grid for wide stencil 17 points, in two dimension.

of the (MAD) in two dimensions. The discretization of the equivalent obtained problem (Method A) is described in Section 4. In Sections 5, we discuss two fixed point problems (Method B and Method C). In Section 6, the methods discussed in the preceding sections are s applied to the solution of test problems.

3. Formulation of the (MAD) in two dimensions

Let us recall the following variant of the AM-GM inequalities: For A and B two symmetric matrices, such that, $A, B \geq 0$. We have the following inequality

$$2\sqrt{\det(AB)} \leq Tr\,(AB)\,.$$

Where for symmetric matrices $M \geq 0$ means $x^T M x \geq 0$.

Remark 3.1. We can deduce from the above that for a smooth convex solution u of (1.1), one can deduce the following inequality

$$\Delta u - 2\sqrt{f} \geq 0.$$

Let us define the function

$$\tilde{g} := \Delta u - 2\sqrt{f}.$$

It is then straightforward to check that if u is a smooth solution of (1.1), then is indeed a solution of the linear Dirichlet Poisson problem

$$\left(\mathcal{P}^{\tilde{g}}\right)\begin{cases}\Delta u = 2\sqrt{f} + \tilde{g},\\ u_{|\Gamma} = \varphi,\end{cases} \tag{3.1}$$

which can be easily descretized by any method of choice if the function $\tilde{g}$ is known.

We finish this remark by mentioning that the convexity constraint is essential to ensure uniqueness (for example, u and $-u$ are both solution of the Monge Ampère equation). For viscosity solution, this constraint can be required by the equation

$$\lambda_1\left(D^2u\right) \geq 0, \tag{3.2}$$

in the viscosity sense, see for instance [25,26], where $\lambda_1\left(D^2u\right)$ is the smallest eigenvalue of the Hessian of u. However, for a twice continuously differentiable function u, the convexity restriction is equivalent to requiring that the eigenvalues of the Hessian, D^2u, are positives, which is approved by considering the solution $u^{\tilde{g}}$ of the linear Poisson Dirichlet problem $\left(\mathcal{P}^{\tilde{g}}\right)$ as we will see in the following.

3.1. An equivalent problem

Let us begin with a simple approach to illustrate the ideas. We can rephrase, for instance, the (MAD) as the following:

$$\begin{cases}\text{Find a positive function } g, \text{ such that,}\\ \det\left(D^2u^g\right) = \lambda_1\left[D^2u^g\right] \times \lambda_2\left[D^2u^g\right] = f,\end{cases} \tag{3.3}$$

where: u^g is the solution of

$$(\mathcal{P}^g)\begin{cases}\quad \Delta u^g = \lambda_1\left[D^2u^g\right] + \lambda_2\left[D^2u^g\right] = 2\sqrt{f} + g,\\ \quad u^g_{|\Gamma} = \varphi.\end{cases}$$

We are now ready to state a first example of our approches.

Lemma 3.1. *Provided the solution, u, of (1.1) is in H^2, there exists a unique positive function $\tilde{g} \in L^2$, such that $u = u^{\tilde{g}}$, where $u^{\tilde{g}}$ is the solution of $(\mathcal{P}^{\tilde{g}})$. Conversely, if $u^{\bar{g}}$ is solution of (3.3) for some $\bar{g} > 0$, then $u^{\bar{g}} = u$.*

Proof. Let u be a solution of (1.1). From the above, one can see easily, that $u = u^{\tilde{g}}$.

Conversely, if $u^{\bar{g}}$ is a solution of (3.3), we can clearly see that

$$\begin{cases}\det\left(D^2u^{\bar{g}}\right) = f > 0,\\ \Delta u^{\bar{g}} \geq 0.\end{cases}$$

It follows that $u^{\bar{g}}$ is convex and satisfies (1.1). □

Remark 3.2. We notice that according to the result in [32], we have equivalence of viscosity and weak solutions for the Poisson problem. This motivates us to build a convergent scheme to the viscosity solution of Poisson problem $\left(\mathcal{P}^{\tilde{g}}\right)$ through the discretization of the (MAD) problem. The viscosity solution $u^{\tilde{g}}$ of $\left(\mathcal{P}^{\tilde{g}}\right)$ will be equivalent to the weak solution of (MAD) problem in the distributional sense.

4. Discretization of the problem (3.3) (method A)

Two discretizations are considered on an uniform cartesian grid.

4.1. The standard finite difference discretization (method A: SFD)

The problem (3.3) can be written as

$$\begin{cases} \text{Find a positive function } g, \text{ such that,} \\ \det\left(D^2 u^g\right) = f, \end{cases}$$

where u^g is the solution of $\left(\mathcal{P}^g\right)$.

The second derivatives are naturally discretized on a regular and uniform cartesian grid as follows:

$$\begin{aligned} D^2_{xx}u_{ij} &= \frac{1}{h^2}\left(u_{i+1,,j} + u_{i-1,j} -, 2u_{i,,j}\right), \\ D^2_{yy}u_{ij} &= \frac{1}{h^2}\left(u_{i,,j+1} + u_{i,,j-1} - 2u_{i,,j}\right), \\ D^2_{xy}u_{ij} &= \frac{1}{4h^2}\left(u_{i+1,,j+1} + u_{i-1,,j-1} - u_{i-1,,j+1} - u_{i+1,,j-1}\right). \end{aligned}$$

4.2. Wide stencils (method A: WS)

Let us consider a regular and uniform cartesian grid and the stencil at the reference point x_0 consist of the neighbors $x_1, ..., x_N$ (as in Figure 1). We can define v_i in polar coordinates by

$$v_i = x_i - x_0 = h_i v_{\theta_i}.$$

We assume that the stencil is symetric and we define the local spatial resolution and the directional resolution respectively by

$$\bar{h}\left(x_0\right) = \max_i h_i$$

and

$$d\theta = \max_{\theta \in [-\pi,\pi]} \min_i |\theta - \theta_i|.$$

First, the problem (3.3) is written as functions of the eigenvalues of the Hessian. We will then start by discretizing λ_1 and λ_2. Hence by a simple substitution we obtain the scheme for (3.3).

We recall that the smallest and the largest eigenvalues of a symmetric matrix can be represented respectively by the Rayleigh-Ritz formula

$$\lambda_1\left[D^2u\right](x) = \min_\theta \frac{d^2u}{d\nu_\theta^2}, \qquad \lambda_2\left[D^2u\right](x) = \max_\theta \frac{d^2u}{d\nu_\theta^2}, \tag{4.1}$$

where $\nu_\theta = (\cos\theta, \sin\theta)$is the unit vector in the direction of the angle θ.

This formulas was used in [26] to build a monotone scheme in two dimension for the (MAD).

We begin by building monotone schemes for λ_1 and λ_2 on a wide stencil uniform grid. These operators are used to give schemes for all formulations in this paper.

We discretize the eigenvalues of the Hessian by the following formula.

$$\lambda_1^{h,d\theta}\left[D^2u^g\right](x)=\min_i\frac{u^g(x+v_i)-2u^g(x)+u^g(x-v_i)}{|v_i|^2}\tag{4.2}$$

and

$$\lambda_2^{h,d\theta}\left[D^2u^g\right](x)=\max_i\frac{u^g(x+v_i)-2u^g(x)+u^g(x-v_i)}{|v_i|^2}.\tag{4.3}$$

Lemma 4.1. *The schemes (4.2) and (4.3) are degenerate elliptic.*

Proof. We follow the same as in [26].

Since each discrete second derivative in the direction v_i is the average of the terms which have the form $u_j^g-u_i^g$, they are non-decreasing in $u_j^g-u_i^g$. Taking a minimum (or maximum) of non-decreasing functions furnishes a non-decreasing function. □

We finally substitute (4.2) and (4.3) in (3.3) to obtain the wide stencil finite difference scheme of (3.3)

$$\begin{cases}\text{Find a positive function } g^i, \text{ such that,}\\ \lambda_1^{h,d\theta}\left[D^2u^{g^i}\right]\times\lambda_2^{h,d\theta}\left[D^2u^{g^i}\right]=f^i,\end{cases}\tag{4.4}$$

with

$$\begin{cases}\lambda_1^{h,d\theta}\left[D^2u^{g^i}\right]+\lambda_2^{h,d\theta}\left[D^2u^{g^i}\right]=2\sqrt{f^i}+g^i,\\ u^g_{|\Gamma}=\varphi.\end{cases}\tag{4.5}$$

Where $f^i=f(x_i)$ and $g^i=g(x_i)$.

Lemma 4.2. *The scheme (4.4) is degenerate elliptic.*

Proof. From the properties of nondecreasing functions, obtained in [26], that if $G:\mathbb{R}^2\to\mathbb{R}$ is a nondecreasing function, and if F_1 and F_2 are degenerate elliptic finite difference schemes, then so is $F=G(F_1,F_2)$. It is also clear that the discretization $f^i=f(x_i)$ and $g^i=g(x_i)$ does affect the ordering properties. We conclude that (4.4) is degenerate elliptic. □

In the following, for simplicity, we omit the index i when there is no ambiguity.

Definition 4.1. We say the scheme $H^{h,d\theta}$ is consistent with the equation (MAD) at x_0 if for every twice continuously differentiable function $\varphi(x)$ defined in a neighborhood of x_0, $H^{h,d\theta}(\varphi)(x_0)\to H(\varphi)(x_0)$ as $h,d\theta\to 0$. The global scheme defined on Ω is consistent if the limit above holds uniformly for all $x\in\Omega$. (The domain is assumed to be closed and bounded).

Lemma 4.3. *The consistency holds for (4.2) and (4.3) and so for (4.4).*

Proof. Let x_0 be a reference point with neighbors $x_1,...,x_N$, and direction vectors $v_i=x_i-x_{0,}$ for $i=1,...,N$, arranged symmetrically, if v_i is a direction vector, then so is $-v_i$. By Taylor series one has

$$\frac{u^g(x_0+v_i)-2u^g(x_0)+u^g(x_0-v_i)}{|v_i|^2}=\frac{d^2u^g}{dv_i^2}+O\left(h_i^2\right).$$

Let M given symetric 2×2 matrix, that we can take it diagonal. Set v_θ a unit vector. It follows from [26] (Lemma 3) that

$$\min_{\theta \in \{\theta_1, \dots, \theta_N\}} v_\theta^T M v_\theta = \lambda_1 + (\lambda_2 - \lambda_1) O\left(\theta^2\right).$$

Which implies that

$$\lambda_1(\varphi)(x_0) - \lambda_1^{h,d\theta}(\varphi)(x_0) = O\left(\bar{h}^2 + (\lambda_2 - \lambda_1) d\theta^2\right)$$

and thus consistency holds for (4.2). Similar argument gives consistency for (4.3) and so for (4.4). □

Theorem 4.1. *Suppose that unique viscosity solutions exist for the equation (3.3) then the finite difference scheme given by (4.4) converges uniformly on compacts subsets of Ω to the unique viscosity solution of the equation.*

Proof. We need to verify consistency and monotonicity. Consistency follows from Lemma 4.3 and monotonicity follows from Lemma 4.2. □

Finally, the scheme yields a fully nonlinear equation defined on grid functions. We perform the iteration (2.1) and by Theorem 2.3 will converge to a fixed point which is a solution of the equation. This approach is used in [26].

5. Two fixed point operators

5.1. The second method (Method B)

Notice that from Lemma 3.1 if u is a solution of (1.1) $u(x,y) = u^{\tilde{g}}(x,y)$ it follows that $\det\left(D^2 u\right) = \det\left(D^2 u^{\tilde{g}}\right)$, where $u^{\tilde{g}}$ is the solution of (3.1) for $\tilde{g} \in L^2$.

By writing

$$\triangle u^{\tilde{g}} = 2\sqrt{f} + \tilde{g} = \sqrt{\left(\Delta u^{\tilde{g}}\right)^2 + 2\left(f - \det\left(D^2 u^{\tilde{g}}\right)\right)}$$

and expanding $\left(\Delta u^{\tilde{g}}\right)^2 = \left(u_{xx}^{\tilde{g}}\right)^2 + \left(u_{yy}^{\tilde{g}}\right)^2 + 2u_{xx}^{\tilde{g}} u_{yy}^{\tilde{g}}$ we have

$$\triangle u^{\tilde{g}} = \sqrt{\left(u_{xx}^{\tilde{g}}\right)^2 + \left(u_{yy}^{\tilde{g}}\right)^2 + 2\left(u_{xy}^{\tilde{g}}\right)^2 + 2f} = 2\sqrt{f} + \tilde{g}.$$

Let us define the operator $Q : L^2(\Omega) \to L^2(\Omega)$ for $\Omega \subset \mathbb{R}^2$ by

$$Q(g) := \sqrt{\left(u_{xx}^g\right)^2 + \left(u_{yy}^g\right)^2 + 2\left(u_{xy}^g\right)^2 + 2f} - 2\sqrt{f},$$

with u^g solution of $(\mathcal{P}^g)$. So, one has

Lemma 5.1. *$\tilde{g}$ is a fixed point of Q.*

Proof. It follows from above expansions. □

5.1.1. The scheme

We consider the following scheme

$$g_{n+1} = Q(g_n) = \sqrt{\left(u_{xx}^{g_n}\right)^2 + \left(u_{yy}^{g_n}\right)^2 + 2\left(u_{xy}^{g_n}\right)^2 + 2f} - 2\sqrt{f}.$$

With initial value $g_0 > 0$ close to zero and u^{g_0} is the solution of (P^{g_0}).

Remark 5.1. The advantage of this method by comparing it to that in [16] and [3] is that it guarantees, at least, at each iteration that $tr\left(D^2u^{g_n}(x)\right) > 0$, which is necessary but of course not sufficient to guarantee convexity at each iteration.

Although this method turns out to be simple to implement is well suited in the case where u^g is in $H^2(\Omega)$. If not, the method may not converge.

5.1.2. Algorithm

- $g_0 \geq 0$ (close to 0), solve (P^{g_0}), $((u^g)^0 = u^{g_0}$being known),
- For $n \geq 0$, compute g^{n+1} and $(u^g)^{n+1}$ as follows

$$g^{n+1} = Q(g^n),$$
$$(u^g)^{n+1} \text{ solution of } \left(P^{g^{n+1}}\right).$$

Where, the method involves simply discretising the second derivatives using standard central differences on a uniform Cartesian grid, as a result

$$\begin{aligned}
D^2_{xx}u_{ij} &= \frac{1}{h^2}\left(u_{i+1,,j} + u_{i-1,j}-, 2u_{i,,j}\right),\\
D^2_{yy}u_{ij} &= \frac{1}{h^2}\left(u_{i,,j+1} + u_{i,,j-1} - 2u_{i,,j}\right),\\
D^2_{xy}u_{ij} &= \frac{1}{4h^2}\left(u_{i+1,,j+1} + u_{i-1,,j-1} - u_{i-1,,j+1} - u_{i+1,,j-1}\right).
\end{aligned}$$

5.2. The third method

In the same setting we define the next operator.

Definition 5.1. Let Ω a bounded domain in $\mathbb{R}^2$. Define the operator $F : L^2(\Omega) \to L^2(\Omega)$, by

$$F(g) = \sqrt{\left|\det\left[D^2u^g\right] - f\right|} + g, \tag{5.1}$$

where u^g is a solution of

$$(\mathcal{P}^g)\begin{cases}\Delta u = 2\sqrt{f} + g,\\ u_{|\Gamma} = \varphi.\end{cases} \tag{5.2}$$

For $g \in L^2(\Omega)$, the operator F is well defined and it is easy to verify that

Lemma 5.2. *$\widetilde{g}$ is a fixed point of the operator F.*

Proof. Let u a smooth solution of (1.1). It follows from Lemma 3.1 that $u = u^{\widetilde{g}}$. Which implies that $\det\left[D^2u^{\widetilde{g}}\right] = \det\left[D^2u\right] = f$ and therefore, $F(\widetilde{g}) = \widetilde{g}$. □

5.2.1. The scheme

We define the following scheme

$$g_{n+1} = F(g_n) = \sqrt{\left|\det\left[D^2u^{g_n}\right] - f\right|} + g_n.$$

With initial value $g_0 > 0$ close to zero and u^{g_0} is the solution of (P^{g_0}).

Remark 5.2. The method is advantageous, it simply involves evaluating derivatives and solving the Poisson equation. As in the previous method, this one turns out to be convenient for u^g in $H^2(\Omega)$, if not, it may not converge.

5.2.2. Algorithm

- $g_0 \geq 0$ (close to 0), solve (P^{g_0}), $((u^g)^0 = u^{g_0}$being known),
- For $n \geq 0$, compute g^{n+1} and $(u^g)^{n+1}$ as follows

$$g^{n+1} = \alpha\sqrt{|\det[D^2 u^{g^n}] - f|} + g^n,$$

with $0 < \alpha < 1$,

$$(u^g)^{n+1} \text{ solution of } \left(P^{g^{n+1}}\right).$$

6. Numerical experiments

The three methods are tested on three different examples (smooth or singular solutions). The discretization is done in the wide stencil Finte Difference method with 17- points (see Figure 1). The number of noeuds meshing is equal to $N * N$ with $N = 31, 45, 63, 89, 127$, the step of meshing $h = L/N$, with L is the length of the side of the rectangular domain Ω. Two convergence tests are defined; the first is $||g^{n+1} - g^n||_\infty$ and the second is $||u^{n+1} - u^n||_\infty$.

The methods are tested for different meshing.

The results we obtained were sufficient to show the efficiency of the methods.

In the **first example** we study the regular solution given by:

$$u(x, y) = \exp((x^2 + y^2)/2) \text{ where } \mathrm{f(x, y) = (x^2 + y^2 + 1)\exp(x^2 + y^2)}.$$

The exact solution of the second example is :

$$u(x, y) = \frac{1}{2}((\sqrt{(x - 0.5)^2 + (y - 0.5)^2} - 0.2)^+)^2$$

where

$$f(x, y) = (1 - \frac{0.2}{\sqrt{(x - 0.5)^2 + (y - 0.5)^2 - 0.2)}})^+.$$

In Figure 2 we show the surface plot of the solution and the total CPU time versus N for the methods A, B and C. The Table1 summarize the obtained numerical errors for different meshing. In this case, the method A (WS) is slightly less accurate compare to the method A (SFD).

The results are in Table 2 and Figure 3. One can see easily that the non-smoothness affects the accuracy.

Finally, we consider a **third example** which is singular at the bord of the domain $\Omega = [0, 1] \times [0.1]$, defined by

$$u(x, y) = -\sqrt{(2 - x^2 - y^2)} \text{ where } \mathrm{f(x, y)} = \frac{2}{(2 - \mathrm{x}^2 - \mathrm{y}^2)^2}.$$

The results are illustrated in Table 3 and Figure 4.

In this last example, the accuracy of the (Method A: WS) is better than the accuracy of the (Method A: SFD) and the other methods. This is due to the non-smooth of the solution.

In the three examples, method C is less accurate than the other methods.

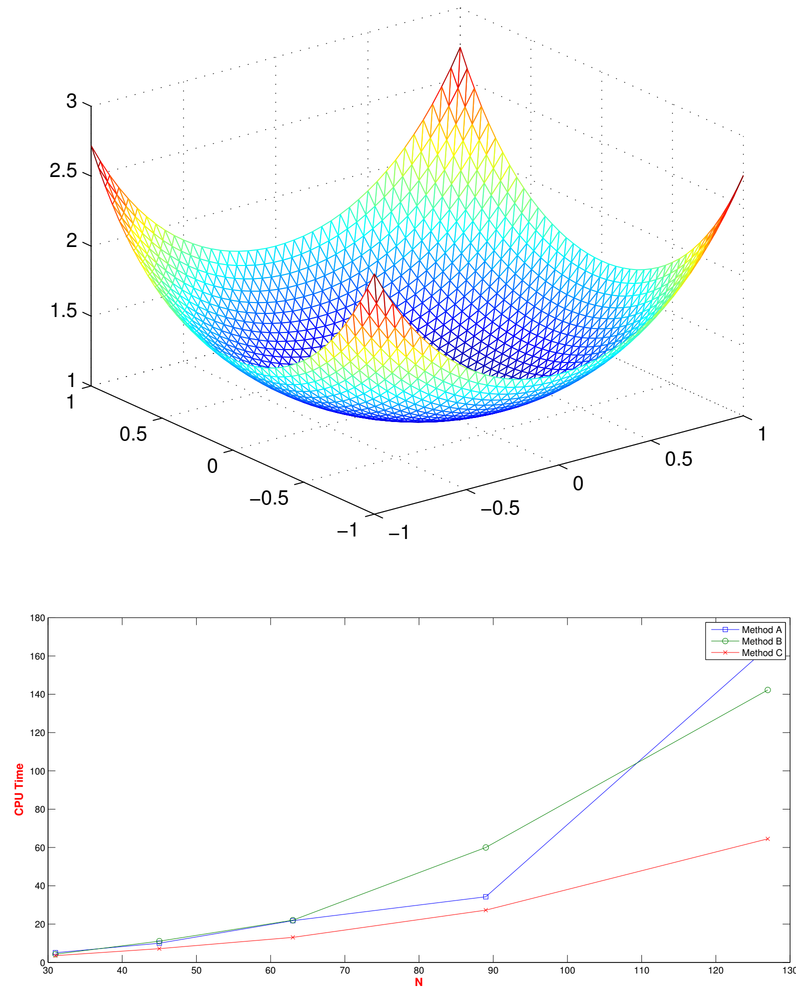

Figure 2. Results for the first example on an $N \times N$ grid and total CPU time versus N for the methods A, B and C.

7. Conclusions

Three numerical methods (A), (B) and (C) for the Dirichlet Monge-Ampère (MAD) equation in two dimensions have been presented.

Computations were performed on a number of examples of varying regularity. Efficiency comparisons were made between the methods and between results available in [16]. In the method (A) two discretization of the equivalent problem are introduced namly (Method A: SFD) and (Method A: WS). The (Method A: SFD) is a discretization with the standard finite difference. The method seems to converge for all the numerical examples and yet this scheme is not monotone and so we can't give a proof of convergence. The second discretization (Method A: WS) is done by wide stencils. Monotone scheme is constructed and convergence is proved.

The Methods B and C are based on introducing a fixed point problems. The

Table 1. Errors $\left\|u - u^N\right\|_\infty$ for the exact solution of the first example on an $N \times N$ grid. We include results from the wide stencil methods of [16] on seventeen point stencils.

N	Method in [16]	Method A: SFD	Method A: WS	Method B	Method C
31	2.44×10^{-4}	7.21×10^{-4}	2.965×10^{-4}	4.226×10^{-4}	18×10^{-4}
45	1.52×10^{-4}	3.41×10^{-5}	3.052×10^{-4}	2.202×10^{-4}	18×10^{-4}
63	9.06×10^{-5}	1.731×10^{-5}	2.801×10^{-4}	1.190×10^{-4}	17×10^{-4}
89	5.32×10^{-5}	1.504×10^{-5}	8.035×10^{-4}	6.494×10^{-5}	17×10^{-4}
127	3.06×10^{-5}	1.321×10^{-5}	2.015×10^{-4}	3.888×10^{-5}	17×10^{-4}

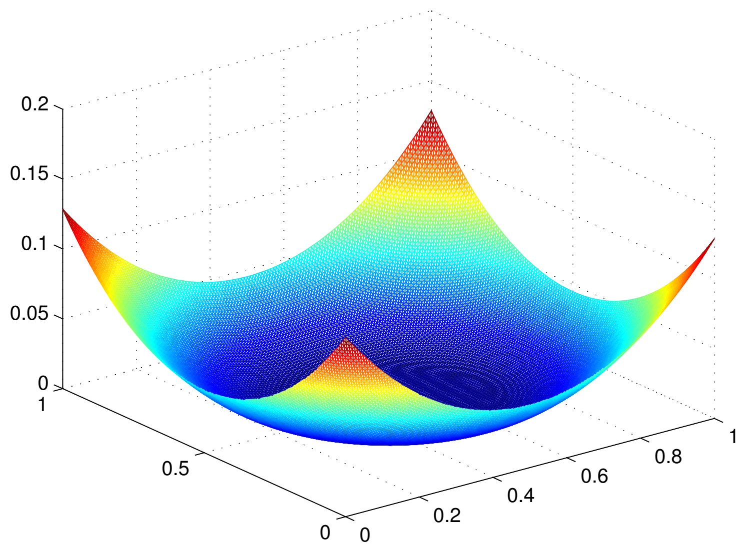

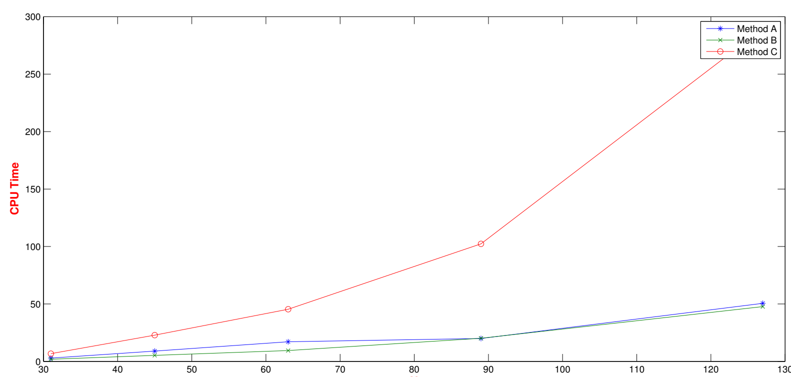

Figure 3. Results for the second example on an $N \times N$ grid and total CPU time versus N for the methods A, B and C.

Table 2. Errors $\left\|u - u^N\right\|_\infty$ for the exact solution of the second example on an $N \times N$ grid. We include results from the wide stencil methods of [16] on seventeen point stencils.

N	Method in [16]	Method A: SFD	Method A: WS	Method B: SFD	Method C: SFD
31	1.22×10^{-3}	5.14×10^{-4}	5.806×10^{-4}	6.853×10^{-4}	8.794×10^{-4}
45	5.9×10^{-4}	5.01×10^{-4}	4.92×10^{-4}	6.719×10^{-4}	8.727×10^{-4}
63	4.2×10^{-4}	4.03×10^{-4}	4.914×10^{-4}	2.733×10^{-4}	8.601×10^{-4}
89	2.6×10^{-4}	3.37×10^{-4}	4.085×10^{-4}	2.09×10^{-5}	8.173×10^{-4}
127	2.0×10^{-4}	3.011×10^{-4}	4.056×10^{-4}	1.08×10^{-5}	8.164×10^{-4}

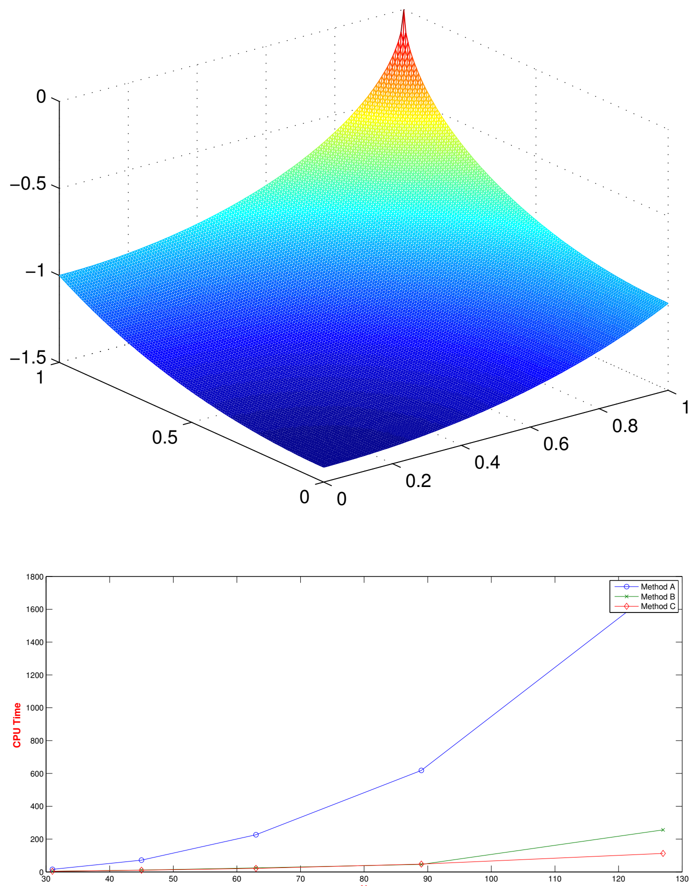

Figure 4. Results for the third example on an $N \times N$ grid and total CPU time versus N for the methods A, B and C.

Method B give more accurate results and seems to converge for regular solutions. However, the Method C is the least accurate since the operator is not regular.

The methods (Method A: WS) and (Method B) have almost the same process time (CPU) in the first two examples where the Method C is the faster in the first example and the slowest in the second example.

Table 3. Errors $\left\|u - u^N\right\|_\infty$ for the exact solution of the third example on an $N \times N$ grid. We include results from the wide stencil methods of [16] on seventeen point stencils.

N	Method in [16]	Method A: SFD	Method A: WS	Method B	Method C
31	1.74×10^{-3}	18.21×10^{-3}	1.7×10^{-3}	5.1×10^{-3}	5.7×10^{-3}
45	9.8×10^{-4}	16.9×10^{-3}	1.5×10^{-3}	4.8×10^{-3}	5.5×10^{-3}
63	5.9×10^{-4}	16.85×10^{-3}	8.9×10^{-4}	3.9×10^{-3}	5.5×10^{-3}
89	3.5×10^{-4}	–	8.9×10^{-4}	3.1×10^{-3}	5.5×10^{-3}
127	2.0×10^{-4}	–	8.2×10^{-4}	2.4×10^{-3}	5.5×10^{-3}

In the third example the (Method A: WS) is the slowest but converges unlike other methods where convergence is not guaranteed, which implies the importance of using the wide stencils for singular solution.

References

[1] G. Barles and P. E. Souganidis, *Convergence of approximation schemes for fully nonlinear second order equations*, Asymptotic Anal., 1991, 4(3), 271–283.

[2] F. B. Belgacem, *Optimization approach for the Monge-Ampère equation*, Acta Mathematica Scientia., 2018, 38(4), 1285–1295.

[3] J. D. Benamou, B. D. Froese and A. M. Oberman, *Two numerical methods for the elliptic Monge-Ampère equation*, ESAIM: Math. Model. Numer. Anal., 2010, 44(4), 271–293.

[4] R. J. Berman, *Convergence rates for discretized Monge-Ampère equations and quantitative stability of optimal transport*, Found Comput. Math., 2021, 21, 1099–1140.

[5] M. W. M. C. Bertens, et al., *Numerical methods for the hyperbolic Monge-Ampère equation based on the method of characteristics*, Partial Differential Equations and Applications, 2022, 52(3), 1–42.

[6] G. Bonnet and J. M. Mirebeau, *Monotone discretization of the Monge-Ampère equation of optimal transport*, ESAIM: M2AN., 2022, 56, 815–865.

[7] C. J. Budd and J. F. Williams, *Moving mesh generation using the parabolic Monge-Ampère equation*, SIAM J. Sci. Comput., 2009, 31(5), 3438–3465.

[8] E. Calabi, *Complete affine hyperspheres. I*, Symposia Mathematica., 1972, 10, 19–38.

[9] S. Y. Cheng and S. T. Yau, *Complete affine hypersurfaces. I. The completeness of affine metrics*, Comm. Pure Appl. Math., 1986, 39(6), 839–866.

[10] E. J. Dean and R. Glowinski, *An augmented Lagrangian approach to the numerical solution of the Dirichlet problem for the elliptic Monge-Ampère equation in two dimensions*, Electron. Trans. Numer. Anal., 2006, 22, 779–784.

[11] E. J. Dean and R. Glowinski, *On the numerical solution of the elliptic Monge-Ampère equation in dimension two: A least-squares approach*, in Partial differential equations, 2008, 16, 887–892.

[12] E. J. Dean and R. Glowinski, *Numerical methods for fully nonlinear elliptic equations of the Monge-Ampère type*, Comput. Methods Appl. Mech. Engrg., 2006, 195(13–16), 1344–1386.

[13] G. L. Delzanno, et al., *An optimal robust equidistribution method for two-dimensional grid adaptation based on Monge-Kantorovich optimization*, J. Comput. Phys., 2008, 227(23), 9841–9864.

[14] X. Feng and M. Neilan, *Mixed finite element methods for the fully nonlinear Monge-Ampère equation based on the vanishing moment method*, SIAM J. Numer. Anal., 2009, 47(2), 1226–1250.

[15] J. M. Finn, et al., *Grid generation and adaptation by Monge-Kantorovich optimization in two and three dimensions*, in Proceedings of the 17th International Meshing Roundtable, 2008, 551–568.

[16] B. D. Froese and A. M. Oberman, *Convergent finite difference solvers for viscosity solutions of the elliptic Monge-Ampère equation in dimensions two and higher*, SIAM J. Numer. Anal., 2011, 49, 1692–1714.

[17] T. Glimm and V. Oliker, *Optical design of single reflector systems and the Monge-Kantorovich mass transfer problem*, J. Math. Sci. (N. Y.), 2003, 117(3), 4096–4108.

[18] C. E. Gutiérrez, *The Monge-Ampère equation*, Progress in Nonlinear Differential Equations and their Applications, 2001, 44, 31–43.

[19] S. Haker, et al., *Mass preserving mappings and image registration*, in MICCAI '01: Proceedings of the 4th International Conference on Medical Image Computing and Computer-Assisted Intervention, 2001, 120–127.

[20] S. Haker, et al., *Optimal mass transport for registration and warping*, Int. J. Comput. Vision, 2004, 60(3), 225–240.

[21] Q. Li and Z. Liu, *Cascadic Newton's method for the elliptic Monge-Ampère equation*, International Journal of Wavelets, Multiresolution and Information Processing, 2020, 18(3), 990–996.

[22] H. Liu, S. Leung and J. Qian, *An efficient operator-splitting method for the eigenvalue problem of the Monge-Ampère equation*, Commun. Optim. Theory, 2022, 1–22.

[23] R. H. Nochetto, D. Ntogkas and W. Zhang, *Two-scale method for the Monge-Ampère equation: Convergence to the viscosity solution*, Mathematics of computation, 2019, 88(316), 1085–1109.

[24] A. M. Oberman, *Convergent difference schemes for degenerate elliptic and parabolic equations: Hamilton-Jacobi equations and free boundary problems*, SIAM J. Numer. Anal., 2006, 44(2), 879–895.

[25] A. M. Oberman, *Computing the convex envelope using a nonlinear partial differential equation*, Math. Models Methods Appl. Sci., 2008, 18(5).

[26] A. M. Oberman, *Wide stencil finite difference schemes for the elliptic Monge-Ampère equation and functions of the eigenvalues of the Hessian*, Discrete Contin. Dyn. Syst. Ser. B, 2008, 10(1), 221–238.

[27] A. M. Oberman and L. Silvestre, *The Dirichlet problem for the convex envelope*, Trans. Amer. Math. Soc., 2010, 363(11), 5871–5886.

[28] V. I. Oliker and L. D. Prussner, *On the numerical solution of the equation* $\frac{\partial^2 z}{\partial x^2}\frac{\partial^2 z}{\partial y^2} - \left(\frac{\partial^2 z}{\partial x \partial y}\right)^2 = f$ *and its discretizations, I*, Numer. Math., 1988, 54(3), 271–293.

[29] G. D. Philippis and A. Figalli, *The Monge-Ampère equation and its link to optimal transportation*, Bull. Amer. Math. Soc. (N. S.), 2014, 51(4), 33–46.

[30] A. V. Pogorelov, *On the improper convex affine hyperspheres*, Geometriae Dedicata, 1972, 1(1).

[31] T. U. Rehman, et al., *3D nonrigid registration via optimal mass transport on the GPU*, Med Image Anal, 2009, 13(6), 931–940.

[32] J. Siltakoski, *Equivalence of viscosity and weak solutions for the normalized* $p(x)$*-Laplacian*, Calc. Var., 2018, 57.

[33] N. S. Trudinger and X.-J. Wang, *The Bernstein problem for affine maximal hypersurfaces*, Invent. Math., 2000, 140(2), 399–422.

[34] N. S. Trudinger and X.-J. Wang, *Affine complete locally convex hypersurfaces*, Invent. Math., 2002, 150(1), 45–60.

[35] N. S. Trudinger and X.-J. Wang, *The affine Plateau problem*, J. Amer. Math. Soc., 2005, 18(2), 253–289.

[36] V. Zheligovsky, et al., *The Monge-Ampère equation: Various forms and numerical solution*, J. Comput. Phys., 2010, 229(13), 5043–5061.